

Progress on Grating Interrogation Schemes Using a Tunable Filter

H Geiger, M G Xu, J P Dakin, N C Eaton[†], P J Chivers[†]

Optical Fibre Group, Department of Electronics & Computer Science, University of Southampton,
Southampton SO17 1BJ, UK; Tel: +44-1703-593088, Fax: +44-1703-593149, E-mail: hg@orc.soton.ac.uk

[†] Westland Aerospace, East Cowes PO32 6RH, UK; Tel: +44-1983-283174, Fax: +44-1983-296489

Abstract

We discuss theoretically and experimentally a wavelength interrogation system for Bragg gratings using an acousto-optic tunable filter (AOTF). The measured resolution of 0.5 pm in 5 Hz bandwidth agrees well with the theoretical analysis.

1 Introduction

Since the initial demonstration of fibre Bragg gratings,¹ there has been much interest in their use as sensors for strain and/or temperature.² Wavelength-encoded measurements with grating sensors are ideal for remote sensing, particularly since they are not influenced by changes in optical power. There is particular interest in using grating sensors for smart structures, where a large number of measurement points need to be interrogated. Gratings can be easily wavelength-division multiplexed (WDM) to provide an array of sensors on a single fibre.

Originally, gratings were interrogated using bulky and expensive laboratory optical spectrum analysers. In the last few years, much research effort has been directed into designing alternative grating interrogation systems that accurately and reliably convert wavelength information into an electrical signal. In all reported interrogation systems, this conversion is realised by optical filters, eg

- 1) a bulk optical filter³ or a wavelength-division coupler⁴
- 2) an interferometer: Mach-Zehnder⁵ or Fabry-Perot (FPI)⁶
- 3) a tunable grating⁷
- 4) an acousto-optic tunable filter (AOTF)^{8,9}

All systems convert wavelength into optical power on the edge of an optical filter. If the filter edge is static, a compromise between high edge slope, ie high sensitivity, and a large interrogation range has to be found. A low sensitivity may be compensated for by increasing the signal strength, eg by using the grating sensors as wavelength-selective mirrors for a laser.^{2,10,11}

This paper discusses design, modelling and experimental results of the first reported system using an AOTF to track the wavelengths of multiple gratings. The system is practical since it uses few optical components, all interconnected with optical fibre without requiring optical alignment. An electronic feedback system provides lock-in operation, and the change of wavelength is displayed on a personal computer (PC). Software on the PC supervises the system operation and allows measurement of both static and dynamic strain.

2 Overview of The Lock-In Technique

The output of a grating interrogation system is conveniently interpreted in terms of the grating wavelength. This interpretation is particularly easy with an AOTF-based approach, since small changes in AOTF wavelength are a linear function of the change in the RF frequency applied to it. RF frequency is a convenient parameter to measure, allowing very accurate measurements with excellent long-term stability.

A tunable filter overcomes the need to trade off sensitivity for interrogation range. With a tunable and symmetric bandpass (or a bandstop) filter, a lock-in technique may be used. To interrogate many gratings by WDM, a large tuning range is desired and offered by both the FPI-based and the AOTF-based approaches. However, the AOTF can be driven at multiple wavelengths simultaneously, allowing in principle a parallel interrogation of many gratings in addition to the TDM offered by using a FPI.

The interrogation system in Fig 1 allows two modes of interrogation: (i) a scan mode and (ii) a lock-in mode. In the scan mode, the feedback loop is disabled and the PC tunes the AOTF via the VCO over the wavelength range

of interest. The power reflected from the gratings is recorded.

In the lock-in mode, the system tracks the wavelength of a particular grating using the feedback loop. The PC initiates a frequency-shift keying (FSK) of the RF signal to the AOTF by driving the VCO with a square wave. This toggles the centre wavelength of the AOTF between two wavelengths within the bandwidth of a selected grating. When the reflected optical power at these two wavelengths is not equal, the detected optical signal is amplitude-modulated at the toggling frequency. Multiplying the detected signal with the toggling signal generates an error signal proportional to the difference between the mean AOTF wavelength and the grating wavelength. This error signal is integrated and used to tune the mean AOTF wavelength to match the grating wavelength. Counting cycles of the AOTF drive signal over integer multiples of the toggling period measures the mean AOTF frequency. The mean frequency gives an accurate measurement of changes in the grating wavelength.

The system may interrogate fibre gratings using either transmissive or reflective optical configurations. This technique may track the wavelength of multiple gratings due to the large tuning range offered by an AOTF (about 1 octave). Gratings at different wavelengths may be either situated along one fibre, or on different fibres. The present interrogation system tracks a single grating at any time, but may switch between many. The switching time between gratings is currently 50 ms.

3 Experimental Results

The system was calibrated by mounting gratings next to resistance strain gauges and applying static loads. The mean AOTF frequency was read and plotted against strain measurements using a commercial resistance strain gauge amplifier.

Fig 2 shows the change of the mean AOTF frequency due to strain applied to an aluminium cantilever beam. The system tracked the grating, and a scale factor of -96.7 Hz/ $\mu\epsilon$ was determined.

The measurement resolution improves when the gating time of the counter is increased. This measurement period may determine the system response, and is software-controlled to allow both fast and slow measurements with the same system. The user interface and real-time measurements have recently been reported.⁹

4 Linear System Model in Lock-in Mode

Around the lock-in point, the optical subsystem can be approximated by a linear change in the power modulation ΔP in response to changes in the grating wavelength λ_G .¹² Therefore the system in Fig 1 may be modelled by a linear system using the grating wavelength as the input value and the mean VCO frequency f_V as the output value (Fig 3). The model predicts the dynamic behaviour and derives a shot-noise-limited resolution.

The optical subsystem, detector, VCO, and AOTF can be modelled with the respective constant gains k_T , k_D , k_V , and k_F , assuming their response times are much faster than that of the integrator.

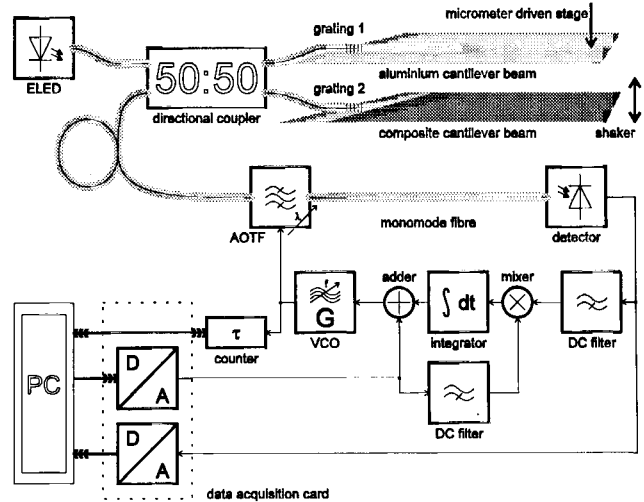


Fig 1 Block diagram of realised grating interrogation system and experimental setup

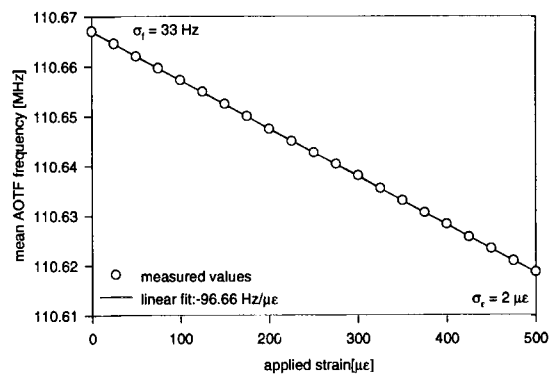


Fig 2 Calibration of AOTF frequency against applied strain: linear fit and standard deviations of strain and frequency measurement

From the model in Fig 3, a transfer function of a first-order system may be obtained:

$$\frac{f_V(s)}{\lambda_G(s)} = \frac{k_T k_D k_I k_V}{s + k_T k_D k_I k_V k_F} = \frac{k_I}{s + \omega_A} \quad [1]$$

where k_I is the forward gain and ω_A is the loop bandwidth.

Even considering noiseless components in the system, shot noise due the quantised nature of light cannot be avoided. The shot noise may be expressed as a current in the detector, or as a noise-equivalent power (NEP):¹³

$$NEP_{sh} = \int_0^\infty NEP_{sh}(f) df = \sqrt{2e_0 \frac{P}{r} B_N} \quad [2]$$

where e_0 is the charge of an electron, P is the mean received power, r is the responsivity of the photodiode, and B_N is the noise-equivalent bandwidth.

Considering the model in Fig 3, the transfer function for the NEP is

$$\frac{f_V(s)}{NEP_{sh}(s)} = \frac{k_D k_I k_V}{s + k_T k_D k_I k_V k_F} = \frac{\frac{k_I}{k_T}}{s + \omega_A} \quad [3]$$

Since this noise transfer function is a first-order lowpass filter, it can be described as being constant at $1/(k_F k_T)$ over its noise-equivalent bandwidth¹⁴

$$B_N = \frac{\pi \omega_A}{2 \cdot 2\pi} = \frac{\omega_A}{4} \quad [4]$$

The standard deviation of the measurement due to the shot noise can hence be computed using Eq [2]

$$\sigma_{IV} = \int_0^\infty \frac{NEP_{sh}(f)}{k_F k_T} df = \frac{NEP_{sh}}{k_F k_T} = \frac{1}{k_F k_T} \sqrt{2e_0 \frac{P}{r} B_N} \quad [5]$$

Equivalently, the measurement accuracy may be expressed in terms of the standard deviation in the wavelength measurement:

$$\sigma_{\lambda G} = \frac{NEP_{sh}}{k_T} = \frac{1}{k_T} \sqrt{2e_0 \frac{P}{r} B_N} \quad [6]$$

This illustrates that for a highly accurate system, the maximum gain k_T in the optical system should be implemented. When the mean optical power affects the noise, eg in a shot-noise limited system, choosing identical bandwidths for grating and AOTF is only approximately optimal since B_G and B_F affect both signal and noise.

The measurement accuracy is optimum for a particular bandwidth ratio B_G/B_F between the grating and the AOTF. Using the optimum wavelength deviation,¹² the measurement accuracy (Eq [6]) is shown in Fig 4. It shows that the optimum ratio is close to 1 in both transmissive and reflective configurations.

The accuracy in both configurations is proportional to the square root of electrical bandwidth B_N and optical

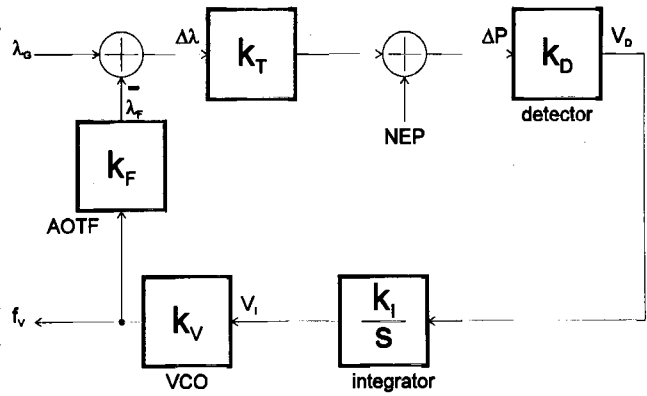


Fig 3 Linear model of system in Fig 1

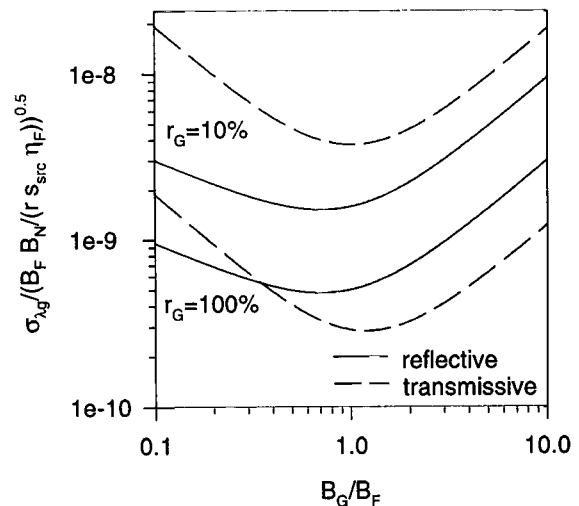


Fig 4 Normalised theoretical resolution of shot-noise limited interrogation system (lower traces: $r_G=100\%$, upper traces: $r_G=10\%$, reflective using ideal 3dB coupler)

bandwidths B_G, B_F . The transmissive configuration delivers the best resolution for high reflectivity gratings of similar bandwidth to the AOTF. However, for low-reflectivity gratings and when the grating bandwidth is much smaller than that of the AOTF, the reflective configuration shows the better noise performance. For a particular ELED (6 μ W over 56 nm) and AOTF, we measured a standard deviation of 0.4 microstrain with $B_N = 5$ Hz. This compares well with a computed shot-noise limited standard deviation of 0.1 microstrain from the above analysis. This theoretical discussion is equally applicable to techniques using other optical filters and will be presented in more detail elsewhere.¹⁵

5 Conclusions

The system monitors the reflective wavelength of a fibre grating and deduces the local strain. For the first time, the wavelength of AOTF has been locked onto the grating wavelength to measure strain. The resulting frequency of the AOTF drive signal is an excellent measurement of the change in grating wavelength. The system has been modelled, and measured standard deviations were within an order of magnitude of the predicted shot-noise-limited accuracy.

Interferometric fibre sensors may also be interrogated with the same system.¹⁶ This approach is also suitable for pressure sensing, particularly when the grating is placed in a glass bubble to achieve greater mechanical compliance.¹⁷

References

1. Meltz G, Morey W W, Glenn W H, "Formation of Bragg gratings in optical fibers by a transverse holographic method", *Optics Letters*, vol 14, no 15, pp 823-825, 1989
2. Morey W W, Meltz G, Glenn W H, "Fiber optic Bragg grating sensors", *Fiber Optic and Laser Sensors VII*, SPIE vol 1169, pp 98-107, 1989
3. Melle S M, Liu K, Measures R M, "A passive wavelength demodulation system for guided-wave Bragg grating sensors", *IEEE Photonics Technology Letters*, vol 4, no 5, pp 516-518, 1992
4. Davis M A, Kersey A D, "All-fibre Bragg grating strain sensor demodulation technique using a wavelength division coupler", *Electronics Letters*, vol 30, no 1, pp 75-77, 1994
5. Kersey A D, Berkoff T A, Morey W W, "High resolution fiber grating based strain sensor with interferometric wavelength shift detection", *Electronic Letters*, vol 28, no 3, pp 236-238, 1992
6. Kersey A D, Berkoff T A, Morey W W, "Multiplexed fiber Bragg grating strain sensor system with a fiber Fabry-Perot wavelength filter", *Optics Letters*, vol 18, no 16, pp 1370-1372, 1993
7. Jackson D A, Lobo Riberio A B, Reekie L, Archambault J L, "Simple multiplexing scheme for a fiber-optic grating sensor network", *Optics Letters*, vol 18, no 14, pp 1192-1194, 1993
8. Xu M G, Geiger H, Archambault J L, Reekie L, Dakin J P, "Novel interrogation system for fibre Bragg grating sensors using an acousto-optic tunable filter", *Electronics Letters*, vol 29, no 17, p 1510f, 1993
9. Geiger H, Xu M G, Eaton N C, Dakin J P, "Electronic tracking system for multiplexed fibre grating sensors", *Electronics Letters*, vol 31, no 12, p 1006f, 1995
10. Melle S M, Alavie A T, Karr S, Coroy T, Liu K, Measures R M, "A Bragg grating-tuned fiber laser strain sensor system", *IEEE Photonics Technology Letters*, vol 5, no 2, pp 263-266, 1993
11. Alavie A T, Karr S E, Othonos A, Measures R M, "A multiplexed Bragg grating fiber laser sensor system", *IEEE Photonics Technology Letters*, vol 5, no 9, pp 1112-1114, 1993
12. Xu M G, Geiger H, Archambault J L, Reekie L, Dakin J P, "Novel frequency-agile interrogating system for fiber Bragg grating sensors", *Distributed and Multiplexed Fiber Optic Sensors III*, SPIE vol 2071, pp 59-65, 1993
13. Smith R G, Personick S D, "Receiver design for optical fiber communication systems", published in: Kressel H, "Semiconductor devices for optical communications", *Springer Verlag*, 1980
14. Stremmler F G, "Introduction to communication systems", 3rd ed, *Addison-Wesley*, pp 195-197, 1990
15. Xu M G, Geiger H, Dakin J P, "Modelling and performance analysis of a fibre-grating interrogation system using an acousto-optical tunable filter", accepted for publication in *Journal of Lightwave Technology*
16. Xu M G, Geiger H, Dakin J P, "Interrogation of fibre-optic interferometric sensors using acousto-optic tunable filter", *Electronics Letters*, vol 31, no 17, p 1487f, 1995
17. Xu M G, Geiger H, Dakin J P, "Fibre grating pressure sensor with enhanced sensitivity using a glass-bubble housing", accepted for publication in *Electronics Letters*